International Journal of Advanced Research in Engineering Technology & Science
ISSN: 2349-2819
Email: editor@ijarets.org Volume-5, Issue-10 October- 2018 www.ijarets.org

EFFECTIVE CALCULATION METHOD FOR EQUIVALENT CIRCUIT VALUES OF SINGLE PHASE INDUCTION DRIVE FED FROM PV INVERTER CONTROLLED BY EXTINCTION ANGLE

Hassan A. Abdul Ghani, Saad S. Eskander
Power and Electrical Machines Department,
Faculty of Engineering, Mansoura University, Egypt

ABSTRACT
This paper is written with the objective of illustrating an effective method to calculate the single phase induction drive equivalent circuit using a steady state tests. The induction drive coupled with photovoltaic (PV) system, this system contains of PV array, inverter, and single phase induction drive. Using a simplified equivalent circuit of a single phase induction drive can be previous directly the machine parameters' calculated with the resistance of core loss is neglected. Especially for the power under the no load test, the equivalent circuit values using the resultant parameter fails to match the input power measured at the drive terminals. However the resistance of core loss included into the calculation framework of drive parameters measurements, the method of Newton Raphson is used to improve calculates obtained by the pattern of direct calculation. So the research has introduced the brief description of a mathematical analysis of this method on the proposed drive. The laboratory experimental results of single phase induction drive demonstrate the effectiveness of an iterative method based the calculation scheme of drive parameters. As using extinction angle for a proposed induction drive model was successfully implemented and tested.

KEYWORDS: Single phase induction drive, parameter measurements, calculation method, PV inverter, and extinction angle

INTRODUCTION
While the single phase induction drive for low power application used widely in domestic utility has never been investigated [1]. During these last years, many research laboratories focused on the variable speed drives, especially for the single phase induction drive, and important renovations have been achieved on this theme [2-3]. Due to the widespread and large energy consumption of single phase induction drives, it is important to improve the techniques of parameter calculation for single phase induction drives, either for monitoring their health condition or to support the power systems operations during fault events [4].

In this paper the performance of a single phase induction drive is connected to a PV system through an inverter is analyzed. Firstly, the mathematical model of the suggested structure is developed. The parameters calculation of single phase induction drive is typically conducted based on measurements collected from the steady state tests. By the direct calculation approach, Ghial et al. have neglected the core loss resistance, which is significantly larger than the impedance of other parameters [5]. Nonetheless, it has been recognized the importance of including the core loss resistance in induction drive modeling [6]. The calculation methods of parameters therein require additional hardware deployment to measure the rotor speed or drive torque. It is more practical to develop advance numerical method that incorporates core loss resistance to fit the steady state tests data at no additional hardware complexity.

Recently, it had developed a non-intrusive approach to calculate induction drive parameters using transient stator current measurements collected during normal start ups by Huynh et al. [7]. Compared to existing test based methods, this approach is more suitable for monitoring the drive capacitor, whose capacitance can decrease gradually throughout the drive lifespan. Nonetheless, the method success in tracking the capacitance value requires a good knowledge of other static drive parameters such as winding resistance, leakage inductance, and magnetizing inductance. Because of the parameter identify ability issue; the time

varying capacitance and the static parameters cannot be determined simultaneously using only transient measurements especially the magnetizing (leakage) inductance. This again speaks for necessary to improving the performance of test based the calculation techniques of induction drive parameters measurements.

Some authors proposed an online parameter calculation, for adaptive systems and self tuning controllers due to the fact that the parameters of induction drive change with temperature, saturation, and frequency [8]. The single phase induction drive is an asymmetrical and coupled machine; these features make the electrical parameter calculation by classical methods difficult, and these characteristics complicate the use of high performance techniques, such as vector and sensor less control. Other studies have also been reported in literature describing the parameter calculation of single phase induction drive [9]. In addition, an equivalent single phase induction drive behavior representation is obtained with the best methodology which has a simple implementation in comparison with the single phase induction drive model obtained by classical tests [10]. Towards this goal, this paper is viewed a calculation pattern of extinction angle of the proposed drive equivalent circuit through developed a calculation methodology of parameters to better fit the power input measurements under various steady state test conditions by incorporating the core loss resistance. With this modification using the Newton Raphson iterative updates is improved the calculations. The objective of the proposed two step method using direct calculations, and Newton Raphson iterations is to further tune up the drive parameters of the equivalent circuit to match the power input measurements. The core loss resistance varies with the slip; our parameters' calculates can potentially be used for modeling the induction drive.

The rest of this research is organized as follows. Section I is illustrated the description of proposed system. Section II is introduced the steady state equivalent circuit model of single phase induction drives. Then the effective method for parameters calculation is developed in Section III. The validation of the proposed method using real measurements is presented, and the experimental results are discussed in Section IV. Finally, the paper is wrapped up with the main conclusion and future scope of this study in Section V.

I. SYSTEM HARDWARE DEVELOPMENT DESCRIPTION

Since the DC/DC and DC/AC power conversion schemes are used, these systems are called dual stage inverters. The DC/DC converter performs maximum power point tracking (MPPT) and inverter converts DC generated by PV to AC. While using dual stage inverter simplifies the control, it decreases the total efficiency of the system and increases the cost. PV systems' cost can be minimized by decreasing the number of power conversion stages and the number of components involved in each stage. In these systems, DC/AC conversion and MPPT processes are performed by same converters; meanwhile this causes an increase in complexity. Furthermore single stage inverters are 4–10% more efficient than the dual stage configurations [11]. In industrial applications, an inverter switching frequency usually varies with the speed of induction drives and the associated error bands, and also it is quite low as compared to the sampling frequency of system. But the variable switching frequency makes very complicate designing of inverter output filter [12].
In this work, the PV system is constituted by a PV arrays, a pulse width modulation (PWM) inverter, and a controlled single phase induction drive to ensure the optimization of the whole system as displayed in Fig.1.

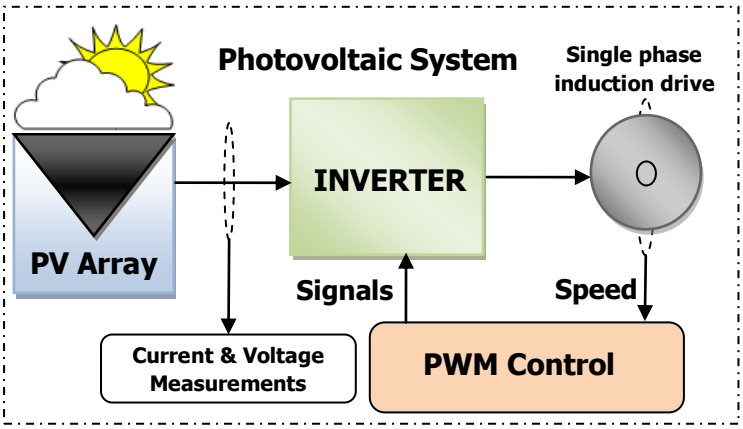

Fig.1: Schematic diagram of the proposed PV system

The PV array is used to generate the DC power and then it is converted into single phase AC power at 50Hz frequency with the help of inverter. The output of the inverter is fed into the single phase induction drive as a load. The characteristic equations of a PV cell can be expressed as [13],

$$I_{SC} = I_L - I_0\left[\exp\left(\frac{qR_S I_{SC}}{nkT_C}\right) - 1\right] - \left(\frac{R_S I_{SC}}{R_P}\right) \quad (1)$$

$$V_{OC} = \frac{nkT_C}{q} ln\left(\frac{I_L + I_0}{I_0}\right) \quad (2)$$

The available values are provided on the PV module datasheet and followed by the parameters to be calculated are tabulated in Table I.

Table I. PV module parameters at STCs of temperature (25°C) and solar irradiation (1000W/m^2)

$\mathbf{I_{MPP}}$	3.595 A	$\mathbf{I_{PV}}$	3.82 A	$\mathbf{I_{SC}}$	3.82 A
$\mathbf{V_{MPP}}$	35.62 V	$\mathbf{I_0}$	0.102 µA	$\mathbf{V_{OC}}$	44.11 V
$\mathbf{P_{MPP}}$	128.1 W	$\mathbf{R_S}$	0.31 Ω	$\mathbf{R_P}$	600 Ω
A	1.2	$\mathbf{k_V}$	-2.10 mV/cell/°C	$\mathbf{k_I}$	15 µA/cell/°C

The circuit structure of whole system for a full bridge single phase inverter as shown in Fig.2. It is an electronic power converter that is necessary as an interface between the power input and the load. The full bridge single phase inverter consists of the DC voltage source, four switching elements Q1, Q2, Q3 and Q4 and load. The used switching element is metal oxide semiconductor field effect transistor (MOSFET). The control of the circuit is accomplished by varying the turn ON time of the upper and lower switch of each inverter leg with the provision of never turning ON both at the same time, to avoid a short circuit of DC bus. The control pulse to the switches is generated by (PIC16F877A) Microcontroller.

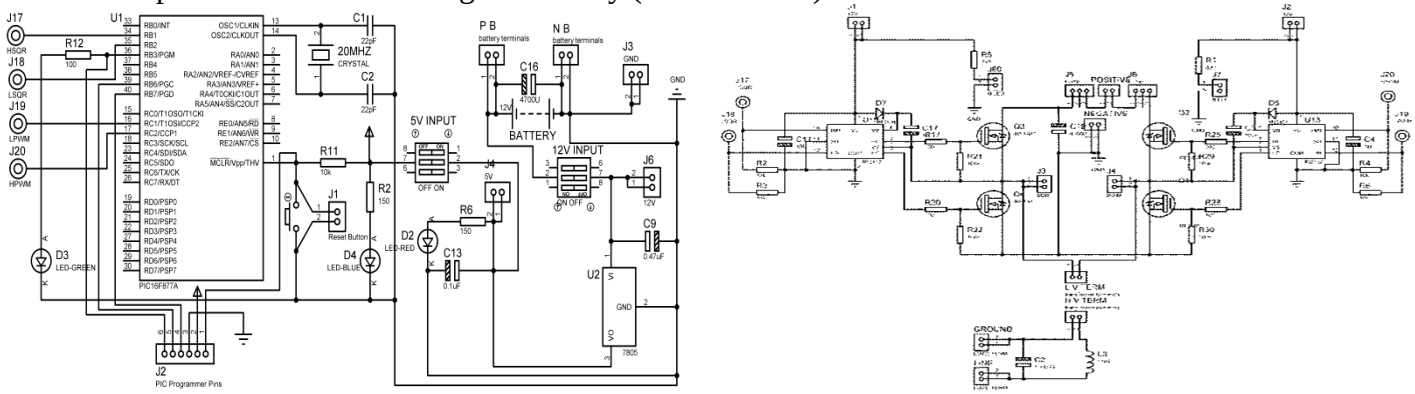

(a) Control circuit (b) Power circuit

Fig.2: The whole system of full bridge single phase inverter circuit topology

A variable voltage is obtained by varying the input DC voltage and maintaining the gain of the inverter constant. On the other hand, if the DC input voltage is fixed then variable output voltage is obtained by varying the gain of the inverter. This is accomplished by PWM control within the inverter. PWM is mean the width of the square pulse in positive and negative halves is adjusted according to the root main square (RMS) of the required output. The inverter gain is defined as ratio of the RMS AC output voltage to DC input voltage. As filter is played a key role in the inverter driven loads. It is eliminated the higher order harmonics. The proposed system layout is allowed the improvement of the efficiency maximization as shown in Fig.1. The need for this configuration is decreased the switching losses, to improve the reliability, and to enhance the converter efficiency.

A prototype laboratory model for a single phase induction drive connected PV system is developed as shown in Fig.3. Various system parameters like voltage and current are measured and conditioned using hall-effect current sensor and isolation amplifier. The control algorithm is first developed in the MATLAB Simulink environment and the MATLAB workshop generated the optimized C code for real time implementation [14]. The interface using Microcontroller is allowed the control algorithm to be run on the system hardware.

Switching signals obtained from the controller are given to the power MOSFETs after proper isolation and amplification. For the testing of the complete prototype, the PV array output is fed to a one level inverter whose output is connected to a single phase induction drive upon parameters measurements change.

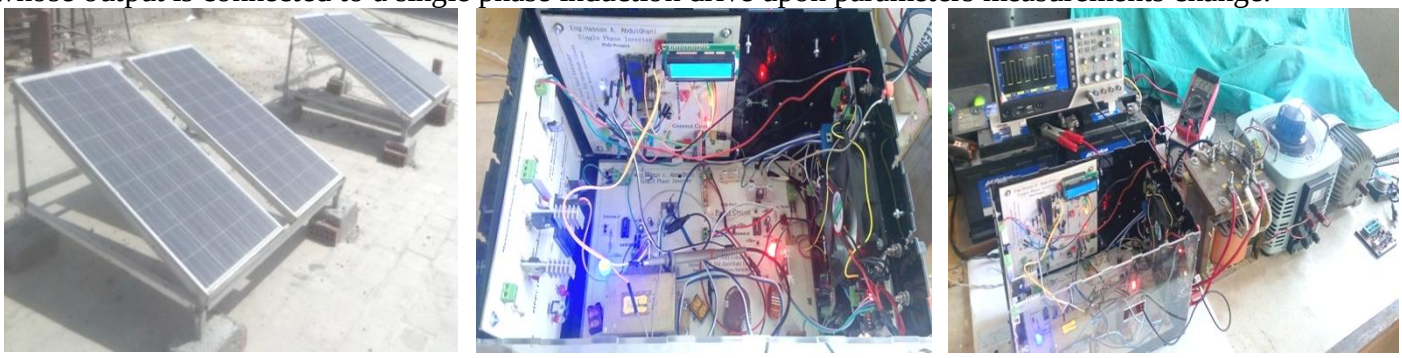

Fig.3: Laboratory prototype model of PV system

II. SINGLE PHASE INDUCTION DRIVE EQUIVALENT CIRCUIT

The commercial single phase induction drive commonly used in low power applications is been a two phase induction machine with asymmetrical windings, whose equivalent circuit without the permanent split-capacitor is represented as in Fig.4. This section is introduced the steady state equivalent circuit for single phase induction drive, which is used in the proposed calculation method of drive parameters. The stator of squirrel cage single phase induction drive had two windings, a main winding and an auxiliary winding, that are placed 90° electrical degrees apart in space. The two windings had different turns number. The external circuit typically is consisted of capacitors with/without a centrifugal switch, is connected in series with the auxiliary winding to enhance the induction drive start-up torque characteristics. The induction drives can be classified into three topology types depending on the external circuit [15].

This paper is focused on the capacitor-start topology because it is the most popular type for residential applications. However, due to the winding arrangement and the single phase sinusoidal power supply, one had to consider two magneto motive force (MMF) waves traveling in opposite directions for each of the stator windings. If only the main winding is connected, the air gap MMF can be decomposed into two traveling waves: one is traveled in the positive rotor angle direction, and the other one is traveled in the negative direction. With sinusoidal current input, the fundamental component of MMF in the air gap F_{ag} at time t and angular position θ can be written as:

$$F_{ag}(t,\theta)=\frac{1}{2}F_0\cos(\omega_e t-\theta+\phi)+\frac{1}{2}F_0\cos(\omega_e t+\theta+\phi) \quad (3)$$

where F_0 is the peak of MMF at the fundamental harmonic in the air gap, ϕ is the phase angle of the main winding current, and ω_e is the electrical frequency (e.g., 120π *rad*/s). The first summand with $\omega_e t-\theta$ is traveled the MMF wave in the positive θ direction with the angular speed, while the other one is traveled the MMF wave in the negative direction at the same speed. Let *s* is the slip between the single phase induction drive rotor's mechanical speed and the MMF wave in the positive direction. It is shown that the slip between the rotor and MMF wave in the negative direction would be $(2-s)$. For each of the MMF waves, the reflected effect of the single phase induction drive rotor on each stator winding. Hence the equivalent circuit of one single phase induction drive winding is consisted of two equivalent circuits of three phase induction drive connected in series with the equivalent parameters scaled by the ($\frac{1}{2}$) factor as described in Fig.4. The top part in the equivalent circuit is corresponded to the MMF wave in the positive rotor angle direction, and thus is termed as the forward branch. Accordingly the bottom part for the MMF in the negative direction is referred as the backward branch. The rest of the paper is displayed the calculation pattern of extinction angle of the proposed drive equivalent circuit through developed the parameters calculation method by accounting for the core loss resistance R_w term with improved performance in fitting the test measurement data. Experimentally the equivalent circuit parameters of an induction drive are found as shown in Fig.4.

III. CALCULATION TECHNIQUE OF PARAMETERS MEASURMENTS

This section is presented the calculation method of parameters using the tests with the main winding connected while the auxiliary winding disconnected for the single phase induction drive equivalent circuit in Fig.4. For the auxiliary winding circuit, one is first disconnected the external capacitor (with C_{st} and R_{st} shorted). This way, the two equivalent circuits is become the same, and the method is presented for only the main winding is directly adopted to calculate the drive parameters.

The effective method goal is found the circuit parameter values in order to match the power measurements of the drive under various test conditions. Certain parameters are directly measured using the dc test such as the main winding resistance R_1. For some of other parameters, including the reactance terms X_1, X'_2 and the magnetizing reactance X_m, as well as the rotor resistance R'_2, one is used additional test measurements to directly calculate a rough estimate of their values. To improve the calculation accuracy, the Newton Raphson method is adopted to fit all the test measurements by iteratively updating the calculations for all these parameters together with the core loss resistance R_w. It is conducted the induction drive tests for this purpose.

A. Single Phase Induction Drive Tests

The following three tests are performed from the collected measurements:

1) DC Stator Resistance Test

The DC stator resistance is directly measured by applying DC current to the main winding terminals and the voltage and current values are taken and are determined the DC and AC resistance as follows, respectively:

$$R_{DC}=\frac{V_{DC}}{I_{DC}} \quad , \quad R_1=1.15\ \mathrm{R_{DC}} \quad (4, 5)$$

2) Blocked Rotor Test

When the rotor is locked from rotation, s_b=s_f=1. An appropriate voltage source is applied to the stator winding such that the proposed drive terminal current is close to its rated value. The secondary impedances become much less than the magnetizing branches and the corresponding equivalent circuit of Fig.5(a).

These test measurements are obtained: blocked rotor power P_{BL}, blocked rotor voltage V_{BL}, and blocked rotor current I_{BL}. Then, equivalent stator resistance R_{Seq}, equivalent stator impedance Z_{Seq}, and equivalent stator reactance X_{Seq} are obtained using the following equations:

$$Z_{Seq}=\frac{V_{BL}}{I_{BL}} \quad , \quad R_{Seq}=\frac{P_{BL}}{(I_{BL})^2}=R_1+R_2^{'} \quad , \quad X_{Seq}=\sqrt{(Z_{Seq})^2-(R_{Seq})^2} \qquad (6,\ 7,\ 8)$$

Separation of X_1, X'_2, R_1, and R'_2 can be done as follows:

$$X_2^{'}=X_{Seq}-X_1 \quad , \quad R_2^{'}=R_{Seq}-R_1 \quad , \quad X_{Seq}=\sqrt{(Z_{Seq})^2-(R_{Seq})^2} \qquad (9,\ 10,\ 11)$$

3) No Load Test

When the induction drive is allowed to run freely at no load, the forward slip s_f is approached zero, (s_f =s) and the backward slip s_b is approached 2, (s_b=2-s). The secondary forward impedance is become very large with respect to the magnetizing branch, while the secondary backward impedance is become very small if compared with the magnetizing branch. Accordingly the equivalent circuit corresponding to these operating conditions are approximated by that of Fig.5(b). The rotor is rotated at the synchronous speed with the assistance of an external mechanical source. The applied voltage source to the stator had at the rated level.

As like the blocked rotor test, same measurements are collected, and are denoted by no load power P_{NL}, no load voltage V_{NL}, and no load current I_{NL}. Then, core loss resistance R_w is obtained as fallows;

$$P_{core+mechanical}=P_{NL}-(I_{NL})^2\left(R_1+\frac{R_2^{'}}{4}\right) \qquad (12)$$

$$\bar{E}_F=\bar{V}_{NL}-\bar{I}_{NL}\left(\left(R_1+\frac{R_2^{'}}{4}\right)+j\left(X_1+\frac{X_2^{'}}{2}\right)\right) \quad , \quad \text{Note:} \quad \left(\bar{I}_{NL}=I_{NL}\angle-\theta,\ \theta=\cos^{-1}\frac{P_{NL}}{V_{NL}I_{NL}}\right) \qquad (13)$$

$$R_w=2\left[\frac{(|E_F|)^2}{P_{core+mechanical}}\right] \qquad (14)$$

and where E_F is electromotive force, the magnetizing reactance X_m is obtained as fallows;

$$I_w=\frac{|E_F|}{\frac{R_w}{2}}=2\left[\frac{|E_F|}{R_w}\right] \quad , \quad I_m=\sqrt{(I_{NL})^2-(I_w)^2} \quad , \quad X_m=2\left[\frac{|E_F|}{I_m}\right] \qquad (15,\ 16,\ 17)$$

or the magnetizing reactance X_m is estimated by;

$$Z_{0eq}=\frac{V_{NL}}{I_{NL}} \quad , \quad X_{0eq}=\sqrt{Z_{0eq}^2-\left(R_1+\frac{R_2^{'}}{4}\right)^2} \quad , \quad X_m=2\left(X_{0eq}-X_1-\left(\frac{X_2^{'}}{2}\right)\right) \qquad (18,\ 19,\ 20)$$

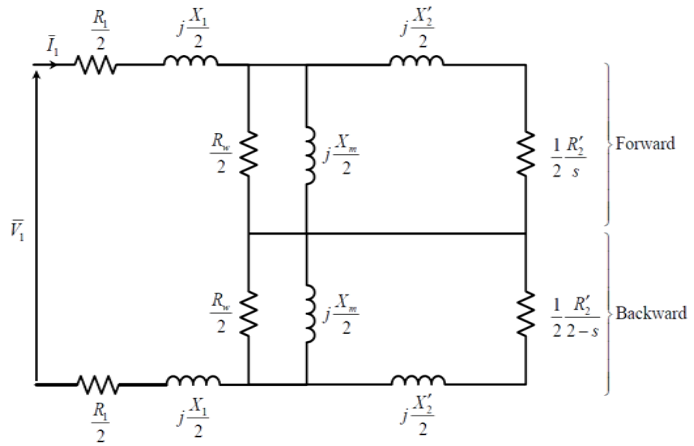

Fig.4: The generalized equivalent circuit of single phase induction drive

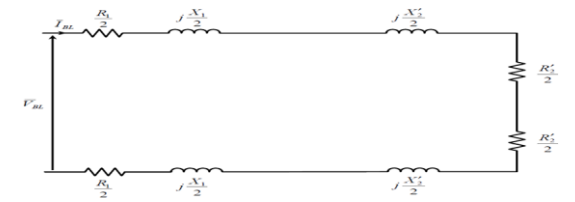

(a) At standstill (blocked rotor)

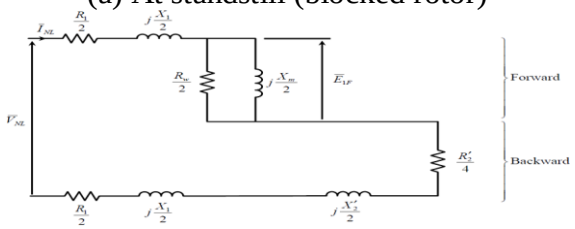

(b) At no load

Fig.5: Approximate proposed drive equivalent circuit

One is simplified the equivalent circuits in Fig.5 under the blocked rotor and no load test conditions. The simplified circuits are made it possible to directly approximate some parameters such as R_l, X_l, X'_2, X_m, and

R'_2. The parameters calculated by this approach are used as the initial guess for the Newton Raphson updates later on. The following assumptions are made to simplify the induction drive equivalent circuits:
• The core loss resistance R_w is significantly larger than the magnetizing reactance X_m. Both of them are much larger than the rotor leakage reactance X'_2 and the rotor resistance R'_2.
• The stator leakage inductance and rotor leakage inductance are the same; i.e., $X_1 = X'_2$.
• There is no coupling between the two stator windings.

Under these assumptions, the simplified equivalent circuit for the blocked rotor test is constructed using the fact that the slip (s=1), as shown by Fig.5(a). The core loss resistance R_w and the main winding magnetizing reactance X_m are eliminated from the simplified circuit. The resultant circuit is consisted of three resistance and three inductance terms, all connected in series. Similarly for the no load test, one is set the slip (s=0) and is constructed the simplified equivalent circuit as illustrated in Fig.5(b). As the rotor effective resistance in the forward branch is been inversely proportional to the slip s and is gone to infinity in this case, the magnetizing reactance X_m part needs to be kept with all other terms are eliminated.

The simplification of the backward branch is followed similarly from the blocked rotor one. The resultant circuit is consisted of two resistance and two inductance terms, all connected in series. Having the simplified equivalent circuits for different tests, the induction drive parameters can be calculated using the direct calculation approach. Although the simplified equivalent circuits are greatly facilitated calculating several of the key parameters, the accuracy of the calculated values is limited by the underlying assumptions [16]. It is observed that the calculations obtained by the direct calculation approach are failed to satisfactorily match the power input measured by all the steady state tests. These calculated values are used as the initial guess for the ensuing Newton Raphson method which can be further tuned up the calculation of parameters.

B. Newton Raphson Method

Specifically, the calculation technique of Newton Raphson method is used to find the parameter values to fit the power measurements collected by the steady state tests. First, the power inputs are represented for blocked rotor and no load tests as a function of all the single phase induction drive parameters. The equivalent circuit in Fig.4 is represented by a single equivalent resistance connected in series with a single equivalent reactance. The equivalent resistance and reactance values under the blocked rotor test and those under the no load test are given in Eqns. (21-24), respectively.

$$R_{BL,eq} = R_1 + \frac{\frac{R'_2}{X_1^2+R_2'^2} + \frac{1}{R_w}}{\left(\frac{X_1}{X_1^2+R_2'^2} + \frac{1}{X_m}\right)^2 + \left(\frac{R'_2}{X_1^2+R_2'^2} + \frac{1}{R_w}\right)^2} \quad , \quad X_{BL,eq} = X_1 + \frac{\frac{X_1}{X_1^2+R_2'^2} + \frac{1}{X_1}}{\left(\frac{X_1}{X_1^2+R_2'^2} + \frac{1}{X_m}\right)^2 + \left(\frac{R'_2}{X_1^2+R_2'^2} + \frac{1}{R_w}\right)^2} \qquad (21, 22)$$

$$R_{NL,eq} = R_1 + \frac{2}{R_w\left(\frac{4}{X_m^2} + \frac{4}{R_w^2}\right)} + \frac{\frac{2}{R_w} + \frac{8R'_2}{4X_1^2+R_2'^2}}{\left(\frac{2}{X_m} + \frac{8X_1}{4X_1^2+R_2'^2}\right)^2 + \left(\frac{2}{R_w} + \frac{8R'_2}{4X_1^2+R_2'^2}\right)^2} \quad , \quad X_{NL,eq} = X_1 + \frac{2}{X_m\left(\frac{4}{X_m^2} + \frac{4}{R_w^2}\right)} + \frac{\frac{2}{X_m} + \frac{4X_1}{4X_1^2+R_2'^2}}{\left(\frac{2}{R_w} + \frac{4R'_2}{4X_1^2+R_2'^2}\right)^2 + \left(\frac{2}{X_m} + \frac{4X_1}{4X_1^2+R_2'^2}\right)^2} \qquad (23, 24)$$

Upon defining these equivalent resistance and reactance terms in Eqns.(21-24), the functional form for power input for each of the tests are become;

$$P_{BL} = (I_{BL})^2 R_{BL,eq} \quad , \quad P_{NL} = (I_{NL})^2 R_{NL,eq} \qquad (25, 26)$$

Accordingly, the function values for the power inputs in the above two equations in (25, 26), the Newton Raphson method is adopted to iteratively update the four unknown variables contained by the vector $x = \left[R_w R'_2 X_1 X_m\right]^T$. Different from the direct calculation approach, the Newton Raphson method is included the core loss resistance R_w as a parameter value to improve the fitting performance. The algorithm of Newton Raphson method is observed typically converges within a dozen of iterations.

C. Extinction Angle Calculation

The fundamental component of input current in extinction angle (β) controlled rectifiers is led the input voltage. Therefore, the displacement factor is led and consequently the power factor is led in extinction angle technique. The extinction angle technique had some improvement over input power factor and the input current total harmonic distortion. This technique is been suitable for most industrial application where speed control of induction drive is required. The used technique to control the extinction angle by use forced commutation nature of the switches while introducing a freewheeling path in parallel with the load terminals. The principle of extinction angle is to start the conduction at the zero crossing of the supply voltage and forced commutated at certain angle before the next zero crossing occurs. The conduction began when switch Q1 is turned on at $t=0$ and is turned off at $t=\pi-\beta$ by force commutation. The freewheeling path for the load current must be provided from $t=\pi-\beta$ to $t=\pi$ by the switch Q2 to discharge the stored energy in the inductance. Thus the fundamental component of input current is led the input voltage and the power factor is led [17]. The output voltage is controlled by the extinction angle β. The average output voltage and the RMS voltage are given by, respectively:

$$V_0 = \frac{V_m}{\pi}\left(\cos(\pi-\beta)+1\right) \quad , \quad V_{rms} = \frac{V_m}{\sqrt{2\pi}}\left[\sqrt{\left\{(\pi-\beta)-\frac{\sin 2(\pi-\beta)}{2}\right\}}\right] \tag{27, 28}$$

The extinction angle is calculated from the following equation;

$$i(\omega t) = \frac{V_m}{Z_T}\left(\sin(\omega t-\phi)+\sin(\phi)e^{-\frac{\omega t}{\tan\phi}}\right) \quad , \text{ where } \quad \phi = \tan^{-1}(\omega t) = \tan^{-1}\left(\frac{\omega L}{R}\right) \tag{29}$$

Starting from $\omega t=\pi$, as ωt increases, the current would keep decreasing. For some value of ωt, say β, the current would be zero. The value of extinction angle β is obtained by substituting $i(\omega t)=0\downarrow_{\omega t=\beta}$,

$$i(\beta) = \frac{V_m}{Z}\left(\sin(\beta-\phi)+\sin(\phi)e^{-\frac{\beta}{\tan\phi}}\right)=0 \tag{30}$$

IV. EXPERIMENTAL RESULTS OF SINGLE PHASE INDUCTION DRIVE

The measurements from steady state tests are used to calculate the parameters in the single phase induction drive equivalent circuit. The effectiveness of the used calculation method of parameters is verified using real measurement data collected from an induction drive in our laboratory. The proposed technique improvements over the direct calculation method are verified from the measurements at different operating conditions. The tested induction drive information on its name plate is listed in Table II.

All measurements under each of tests with main or auxiliary winding connected are recorded in Table III. For each test, the applied voltage and winding current are kept at a rated value. Parameters values are first calculated using the direct calculation approach, and improved using the Newton Raphson method later on.

To validate the accuracy of each set of parameters calculates, their corresponding parameters are computed, as tabulated in Table IV. Compared with the direct calculation results; the Newton Raphson based calculates are more significantly different in the rotor resistance R'_2 and the stator winding inductance X_m. The calculated core loss resistance values by the Newton Raphson method are indeed quite large compared to other parameters. As Table V views the Newton Raphson calculates result in perfect match in terms of input power with the actual measurements, significantly outperforming the results obtained by the direct calculation approach. The latter had experienced much larger mismatch with the power measurement under the no load test. Although it is been reasonable to neglect the core loss resistance as corroborated by its large value, it is truly necessary to include this term for better fitting the drive terminal power measurements under

various steady state tests conditions. The error performance of Newton Raphson method is illustrated in Fig.6, which is plotted the residual norm versus the iteration. Residual norm of the initial guess is plotted at iteration zero. The algorithm is achieved satisfactory error norm within just 3-4 iterations of Newton Raphson updates. As the actual inverter output voltage is seen to track the reference faithfully from a time of about 20 m second. The import of this reference tracking is shown in Fig.7.

Table II. Details of single phase induction drive name plate

PHASE	SINGLE	**TIME RATING**	CONT
POWER	1/3 HP	**VOLTAGE**	230 V
CURRENT	2.8 A	**FREQUENCY**	50 Hz
SPEED	3450 RPM	**CAPACITOR**	20 µF
TYPE	NEMA DESIGN	**AMBIENT TEMP.**	40°C
CODE	L	**INSULATION CLASS**	B

Table III. Blocked rotor and No load test measurements

	Blocked Rotor Test		No Load Test	
Parameter	***Main winding***	***Auxiliary winding***	***Main winding***	***Auxiliary winding***
***V* [V]**	**31.4**	**53.5**	**118.7**	**118.4**
***I* [A]**	**5.5**	**4.9**	**4.5**	**2.6**
***P* [W]**	**105.1**	**227.1**	**85.8**	**78.2**

Table IV. The tested drive parameters with winding

		Parameter					
Calculation Technique		R_1	R'_2	R_w	X_m	X_1	X'_2
Main	***Direct Calculations***	**1.705**	**1.784**	**--**	**123.16**	**6.016**	**6.016**
	Newton Raphson iteration	**1.705**	**1.965**	**488.56**	**122.43**	**6.087**	**6.087**
Aux.	***Direct Calculations***	**6.098**	**3.279**	**--**	**220.91**	**7.287**	**7.287**
	Newton Raphson iteration	**6.098**	**3.514**	**684.18**	**216.12**	**7.258**	**7.258**

Table V. The input power with steady state tests

	Blocked Rotor Test		No Load Test	
Calculation Technique	***Main winding***	***Auxiliary winding***	***Main winding***	***Auxiliary winding***
Measured value	**105.1**	**227.1**	**85.8**	**78.2**
Direct calculations	**100.07**	**222.01**	**41.97**	**45.69**
Newton Raphson iterations	**105.03**	**227.14**	**85.72**	**77.91**

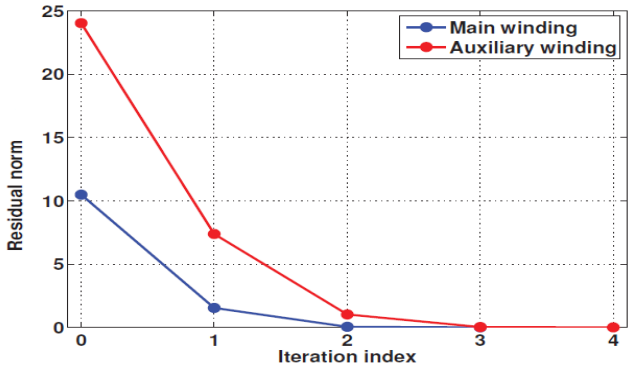

Fig.6: Iterative residual error norm for the drive

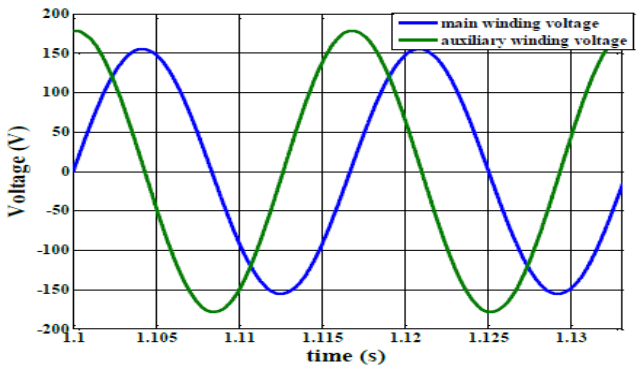

Fig.7: Main and auxiliary winding voltages in two

winding tests Periods

The value of β can be obtained from the equation (30) by substituting for $i(\beta)=0$. Then by using the simple iteration method, the different values of β are substituted in the region $\pi<\beta<2\pi$ till the minimum value of delta is got at corresponding value of β is the required value, [$\Delta = 20.9361\sin(\beta - 0.53288) + 10.63587e^{-1.696\beta}$].
According to this formula, β is found to be (1.16993π) *rad* which is equivalent to (210.7)°. The functional relationship between the extinction angle and the output voltage is obtained using MATLAB programming tool as displayed in Fig.8.

Microcontroller is used to trigger the switch to obtain the extinction angle waveform. The extinction time should be larger than the switch turn OFF time. The switch model and the variations of current and voltage are shown in Fig.9. Regarding switching losses, the turning ON and OFF of the switch should be taken into account, as in both cases voltages and currents appear at the same time, resulting into losses. The most important problem to be considered is the dead time control. Dead time period must be suitable to avoid the switch damaging and harmonic problem. Finally, Extinction angle has better total harmonic distortion (THD) of load current than firing angle because of the continuous load current for inductive load circuit. As Figures 10, 11 are illustrated the switching pulses synchronized with the supply voltage and the output voltage is controlled by varying the extinction angle β, respectively.

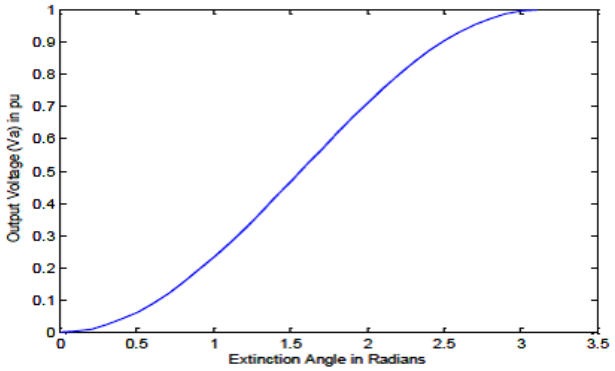

Fig.8: Output voltage vs. extinction angle characteristic

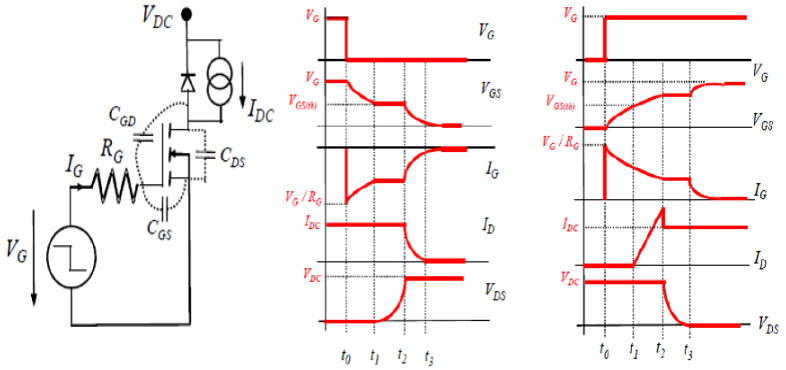

Fig.9: The switch model and waveforms of turning ON and OFF

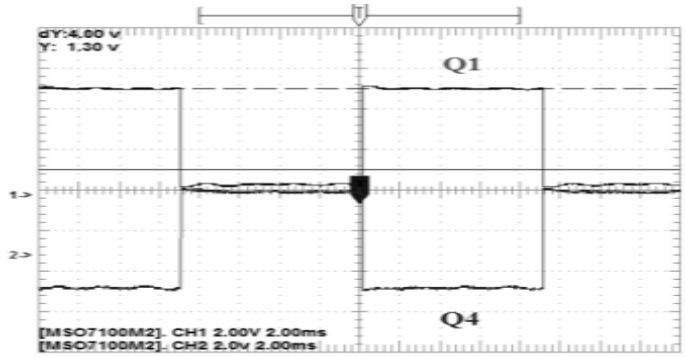

Fig.10: Switching pulses with input voltage

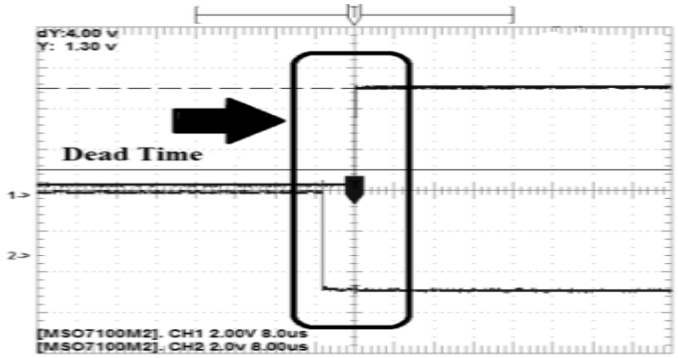

Fig.11: Dead time Representation in control signal

V. CONCLUSION AND FUTURE SCOPE

The aim of this paper is examined the possibility of utilizing a PV array to supply a single phase induction drive through a full wave bridge inverter. We can be concluded that a contribution to the PV system analysis with an effective method to calculate the extinction angle from the single phase induction drive parameters

measurements. However an extinction angle had been developed that the speed control of single phase induction drives. As consequence it is possible to design a high performance single phase induction drive controllers. Here, the single phase induction drive behavior representation is obtained with calculation methodology in comparison with the used drive model parameters measurements obtained by steady state tests. The calculated values had been used by the direct calculation approach. The parameter calculation problem without neglect the core loss resistance is solved using the Newton Raphson calculation method.

The experimental validation in order to checking the analytical results obtained. A laboratory results are demonstrated that the effective calculation method is improved the power measurements fit upon the direct calculation ones at loading change. The single phase induction drive performance during start-up time may be investigated as the future work. With possibility the system hardware setup and its circuit topology analysis may be considered.

REFERENCES

1. Ivana Z., Vasilija J., Saso A., and Vlatko T.: "Single phasing of three phase induction motors under various load conditions", 23rd Int. Scientific-Professional Conference on IT, IEEE, Montenegro, (2018).
2. Deepa M.: "Design of VFD drive for a 3-Phase induction motor", International Journal of Innovative Research in Science, Engineering and Technology (IJIRSET), vol.4, issue.1, pp.18755–18762, (2015).
3. Rong Ching Wu, Yuan Wei Tseng, and Cheng Yi Chen: "Estimating parameters of the induction machine by the polynomial regression", Applied Sciences, MDPI, 8, 1073, (2018).
4. North American Electric Reliability Corporation: "A technical reference paper fault induced delayed voltage recovery", Technical Report, NERC, (2009).
5. Ghial V., Saini L., and Saini J.: "Parameter estimation of permanent-split capacitor-run single phase induction motor using computed complex voltage ratio", IEEE Transaction on Power Electronics, vol.61, no.2, pp.682–692, (2014).
6. Tekgun B., Sozer Y., and Tsukerman I.: "Modeling and parameter estimation of split single phase induction motors", in Proc. IEEE Energy Conversion Congress Exposition, pp.1317–1324, (2014).
7. Huynh P., Zhu H., and Aliprantis D.: "Non-intrusive parameter estimation for single phase induction motors using transient data", in Proc. IEEE Power and Energy Conference at Illinois (PECI), Urbana, (2015).
8. Hrabovcova V., Kalamen L., Sekerak P. and Rafajdus P.: "Determination of single phase induction motor parameters", Int. Sym. on Power Electron. Elec. Drives Auto. and Motion (SPEEDAM), pp.287–292, (2010).
9. Myers M., Bodson M., and Khan F.: "Determination of the parameters of non symmetric induction machines", Annual IEEE Applied Power Electronics Conf. and Expo. (APEC), pp.1028–1033, (2011).
10. Pyne M., Chatterjee A., and Dasgupta S.: "Speed estimation of three phase induction motor using artificial neural network", Inter. Journal of Energy and Power Engineering, vol.3, no.2, pp.52–56, (2014).
11. Patel H., and Agarwal V.: "MPPT scheme for a PV fed single phase single stage grid connected inverter operating in CCM with only one current sensor", IEEE Trans. on Energy Conv., vol.24, pp.256–263, (2009).
12. Pimkumwong N., Onkrong A., and Sapaklom T.: "Modeling and simulation of direct torque control induction motor drives via constant volt/hertz technique", Procedia Eng., vol.31, pp.211–1216, (2012).
13. Mircea Taciuc: "PV cells I–V characteristic explicit equation with three parameters and its simplified forms", 10th International Symposium on Advanced Topics in Electrical Engineering (ATEE), IEEE, (2017).
14. Jigar Mehta: "Simulation of various modulation strategies for induction motor drive" Master Thesis, Department of Electric Drives and Traction, Czech Technical University, (2018).
15. Huynh P., Zhu H., and Aliprantis D.: " Parameter estimation for single phase induction motors using test measurement data", in proceeding of IEEE Power and Energy Conference at Illinois (PECI), Urbana, (2016).
16. Naimuddin S., Tutakne D., and Daigawane P.: "Enhancing power factor with power saving in induction motor drive", International Research Journal of Engineering and Technology (IRJET); vol.2, issue.4,(2015).
17. Akashay B., Amol S., Minakshi P., and Priyanka P.: "Single phase self-excited induction generator", International Journal of Industrial Electronics and Electrical Engineering (IJIEEE), vol.5, issue.2, (2017).